ELSEVIER

Thermochimica Acta 311 (1998) 173–181

thermochimica acta

Thermal, spectroscopic and kinetic characterization of reaction products of copper(II) chloride with photoproducts of octacyanocomplexes of Molybdenum(IV) and Tungsten(IV) with ethylenediamine

S.I. Ali*, Kowsar Majid

Department of Chemistry, Jamia Millia Islamia, New Delhi-110 025, India

Received 11 August 1997; received in revised form 25 November 1997; accepted 3 December 1997

Abstract

The thermal dissociation of complexes formed by copper(II) chloride with photoproducts of $\mathrm{M(CN)_8^{4-}}$ [where M=Mo or W] and ethylenediamine has been studied by thermogravimetry (TG), differential scanning calorimetry (DSC) and IR spectroscopy. The observed IR bands for different groups support the assigned composition. Both Mo(IV) and W(IV) show the same stoichiometric behaviour towards complex formation but a different decomposition behaviour. In case of Mo(IV) decomposition takes place in four steps with cyanide and oxide of copper and tetrachloro molybdenum(IV) as residue, while in case of W(IV) the decomposition occurs only in three steps up to 298°C. The copper cyanide along with tetrachloro tungstate(IV) is found as residue. DSC for Mo complex displays four transitions, two exothermic and two endothermic. In case of W, DSC displays three endothermic transitions corresponding to three decomposition steps with three different ΔH values. On the basis of TG and DSC, mechanism for decomposition of each complex has been proposed. Kinetic parameters like activation energy (E_a), frequency factor (A), entropy of activation ($\Delta S^{\#}$) for each step has been calculated involving differential methods like Doyle, Coats and Redfern and Arrhenius. The heat of the reaction is obtained from DSC curves.

Keywords: Thermal kinetics; Octacyanomolybdate(IV); Octacyanotungstate(IV); Ethylenediamine; Copper(II) complexes

---

1. Introduction

Study of copper(II) complexes is quite interesting because it is biologically active in its chelating ability and its positive redox potential allows it to participate in biological transport reaction [1]. Its complexes possess a wide biological activity and are among the most potent antiviral, antitumor and antiinflammatory agents [2]. These biological activities have promoted the structural activity correlations of its complexes [3–7]. On the other hand the thermal behaviour of chromium, molybdenum and tungsten in their mixed ligand complexes containing carbonyl and pyridine [8] and also carbonyl and triphenyl phosphine [9] have been reported. Since $\mathrm{K_4M(CN)_8}$ (M=Mo or W) is thermally inert but photochemically active, as a result of which photoexcitation of $\mathrm{M(CN)_8^{4-}}$ involves substitution of cyanide ion by different entering ligands, the thermal study of which have been reported [10–15]. Likewise $\mathrm{M(CN)_8^{4-}}$ is

---

*Corresponding author. Fax: 00 91 682 1232.

PII S0040-6031(97)00476-0

reported to form substitution products with ethylenediamine [16], but the complex formation and thermal study of its substituted complexes is not reported so far. In this paper we report the thermal study of complex formation between copper(II) chloride with the photochemically substituted octayanomolybdate(IV) and -tungstate(IV) with ethylenediamine. The kinetics and mechanism along with the thermodynamic parameters viz. activation energy, frequency factor and entropy of activation have been calculated.

2. Experimental

$K_4M(CN)_8$ [where M=Mo(IV) or W(IV)] was prepared by the literature method [17]. AR grade Copper(II) chloride and ethylenediamine were provided by BDH. All the solutions were prepared in doubly distilled water. An ultra-vitulax lamp was used for irradiation purpose.

Synthesis of the chloride complex of copper(II) with the photoproduct of $K_4M(CN)_8$ [where M=Mo(IV) or W(IV)] and ethylenediamine was carried out by irradiating equimolar aqueous solution of $K_4M(CN)_8$ and ethylenediamine under UV light till the solution turned red. To this solution aqueous solution of $CuCl_2$ was added till the precipitation was complete. The precipitates were washed with water and ethanol and dried over fused $CaCl_2$. The complexes were analysed for C, H and N and assigned the formula:

$Cu_2[Mo(CN)_2(OH)_2(C_2H_8N_2)(H_2O)_2]Cl_4$ I for which the observed C, H and N is 8.83%, 3.00% and 10.30% respectively against calculated values as 8.77%, 2.57% and 10.22% respectively. For the complex $Cu_2[W(CN)_2(OH)_2(C_2H_8N_2)(H_2O)_2]Cl_4$ II, the observed percentages are 7.40, 9.05, 2.50 against the calculated 7.56, 8.82, 2.22 for C, H and N respectively.

2.1. Physical measurements

Determination of carbon, hydrogen and nitrogen was carried out by micro analytical methods. The IR spectra of the solid complexes were recorded on Perkin-Elmer (S.No. 782) IR Spectrophotometer in the range of 400–4000 cm^{-1} using KBr disc technique.

2.2. Thermal analysis

Thermogravimetry was performed on Du Pont thermal analyser-2000. The analysis was made in a dynamic nitrogen atmosphere with a rate of 50 ml/min between 30°C and 800°C at a heating rate of 10°C/min. A platinum pan was used. Differential scanning calorimetry was also carried out on a TA analyser (Du Pont TA-2000) with a DSC. The scanning rate was 10°C/min. Temperature range was from room temperature to 500°C. An aluminium pan was used under a dynamic nitrogen atmosphere. The instrument calibration was done by indium (99.99% purity). The temperature repeatability of the instrument is ±0.1°C and of ΔH is ±0.02 mW.

3. Results and discussion

The synthesised complex I was analysed for C, H and N on the basis of which empirical formula was assigned. Further characterization was done by IR spectroscopy. The measured infrared spectra are in conformity with the composition of the complexes and reveal the presence of individual functional groups. The presence of the molecule of ethylenediamine and CN is demonstrated by several characteristic absorption bands. The strong absorption peaks for the complex I at 3400, 1680–1600, 1500 and 1362 cm^{-1} are assigned as $\nu(OH)$, $\nu(C\text{–}N)$, $\nu(NH_2)$ and $\nu(CH_2)$ respectively. The strong and sharp absorption in the region of 2100 and 2200 cm^{-1} for Mo(IV) and W(IV) respectively are due to stretching vibrations of $\nu(C{\equiv}N)$. The band at 2100 cm^{-1} for Mo implies the coordination of the terminal cyanide. Moreover, the absorption of the type $\nu(C\text{–}N)$ and $\nu(NH_2)$ are observed in the region of 1040 and 640–660 cm^{-1} respectively. For complex II, the absorption bands of $\nu(OH)$, $\nu(C{\equiv}N)$, $\nu(C\text{–}N)$, $\nu(CH_2)$ appear on the same frequencies as that of complex I. The appearance of $\nu(NH_2)$ band shows a shift of 80 cm^{-1} from that of Mo towards higher energy. Shifting of N–H vibrations towards the lower frequencies indicate the coordination of nitrogen atom of the amine group to metal atom [18].

3.1. Ta studies

3.1.1. $Cu_2[Mo(CN)_2(OH)_2(C_2H_8N_2)(H_2O)_2]Cl_4$ I

The TG and DTG curves of I are shown in Fig. 1. The DTG curve indicates four different mass loss ranges. The first mass loss is a brief one occurring from 78°C to 100°C is due to the loss of one mole of H_2O. This step is followed by a similar type of transition from 134°C to 142°C with a DTG maximum of 138.7°C due to the removal of another mole of water. The third stage involves a significant mass loss extending from 181°C to 223°C with DTG maximum of 191.3°C corresponding to the removal of 1 mol of ethylenediamine and one mole of hydroxide ion. The fourth and the last stage occurs between 326°C and 343°C and involves the loss of another mole of hydroxide alongwith one mole of cyanide. This stage is observed in DTG peak at 341.0°C The observed mass loss at each decomposition step corresponds to the calculated values (Table 1). The DSC of I displays a respective transition for each transition observed in TG curve with different ΔH values with uncertainty of ± 0.02 (Fig. 2). The first two steps as seen from TG curve involving loss of water corresponds to an overlapping endothermic peak in DSC in the temperature range of 104°C to 192°C with maximum at 144.4°C giving ΔH=57.2 J/g. This endothermic peak is followed by a sharp exothermic peak at 227°C which is due to evolution of ethylenediamine molecule with an enthalpy change ΔH of 31.5 J/g. The decomposition of the remaining complex gives two peaks, one exothermic with maximum at 263°C which is due to the release of two moles of OH groups with ΔH=7.8 J/g. The last step leading to final residue corresponds to an endothermic peak of maximum 384.7°C due to the release of one mole of cyanide molecule. The ΔH value observed is higher as compared to rest of the steps. On the basis of these studies, following scheme may be proposed for thermal decomposition of I. The percentages with and without

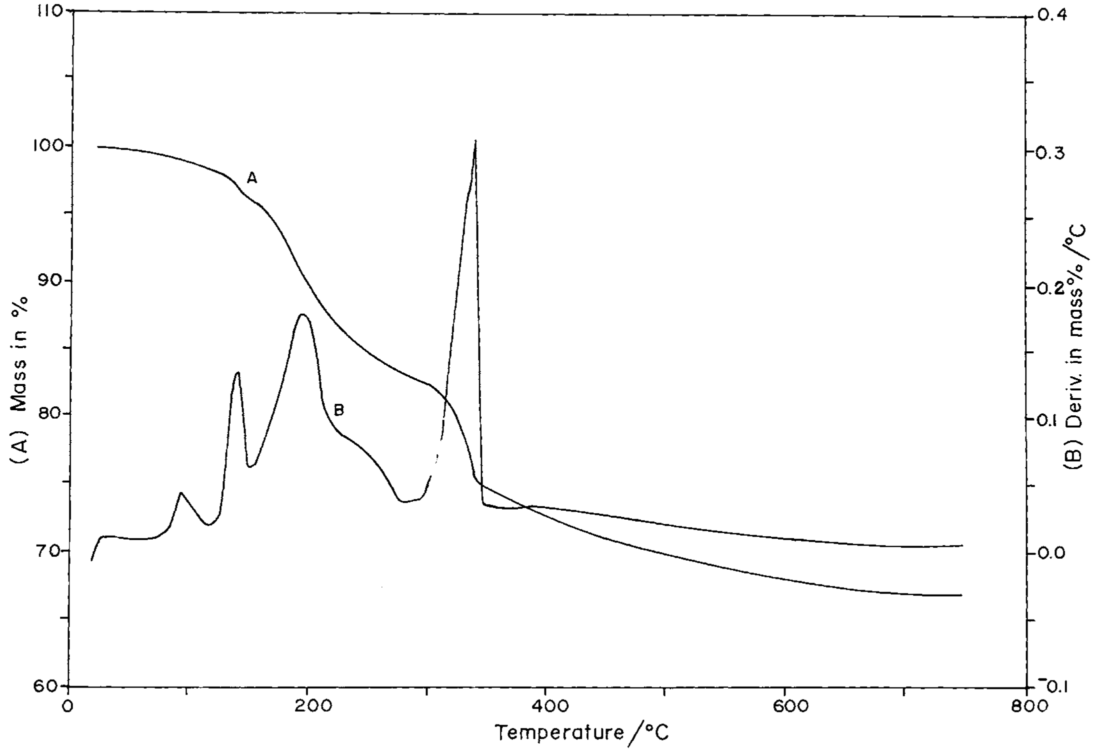

Fig. 1. The TG and DTG curves of complex I.

Table 1
Thermoanalytical data for the decomposition of the complexes:$Cu_2[Mo(CN)_2(OH)_2(C_2H_8N_2)(H_2O)_2]Cl_4$ I $Cu_2[W(CN)_2(OH)_2(C_2H_8N_2)(H_2O)_2]Cl_4$ II

Temp.range in °C	Max. temp. in DTG in °C	Obsd. weight loss in %	Calc. weight loss in %	Remarks removal of
Complex I				
78–100	92.0(1)	2.00	3.2	1 mol of H_2O
136–141	138.7(1)	2.40	3.2	1 mol of H_2O
181–223	191.3(1)	13.5	14.0	1 mol of $C_2H_8N_2$ +1 mol of OH
326–343	341.0(1)	7.83	7.85	1 mol of OH +1 mol of CN residue is CuCN +CuO + $MoCl_4$ calc.(74.28) obsd.74.27%
Complex II				
141–160	147.5(1)	12.16	12.28	1 mol of H_2O +1 mol of $C_2H_8N_2$
247–261	255.5(1)	3.47	2.83	1 mol of H_2O
278–301	289.4(1)	4.38	5.35	2 mol of OH residue 2CuCN+WCl_4 calc. (79.51) obsd. 79.39%.

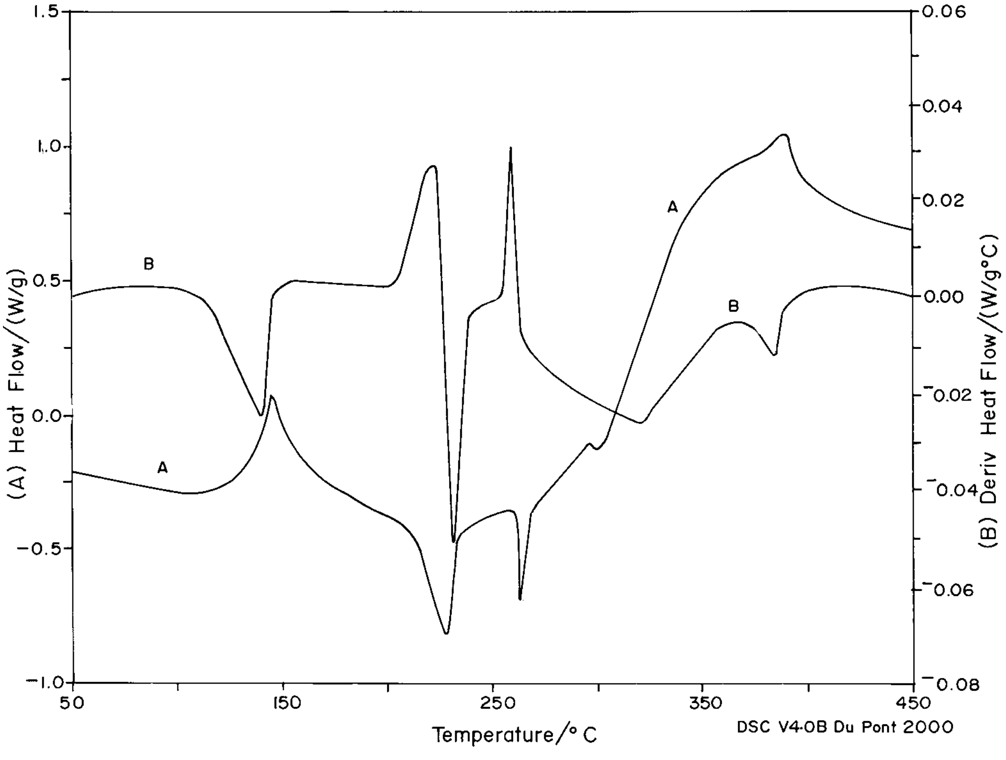

Fig. 2. The DSC curve of complex I.

parentheses correspond to the calculated and observed values respectively.

Scheme I

$$Cu_2[Mo(CN)_2(OH)_2(C_2H_8N_2)(H_2O)_2]\,Cl_4 \xrightarrow[2.0]{(3.2)}$$

$$Cu_2\,[Mo(CN)_2(OH)_2(C_2H_8N_2)(H_2O)]\,Cl_4 + H_2O \xrightarrow[2.4]{(3.2)}$$

$$Cu_2\,[Mo(CN)_2(OH)_2(C_2H_8N_2)]\,Cl_4 + H_2O \xrightarrow[13.5]{(14.0)}$$

$$Cu_2\,[Mo(CN)_2(OH)]\,Cl_4 + OH + C_2H_8N_2 \xrightarrow[7.83]{(7.85)}$$

$$CuCN + \mathrm{CuO} + MoCl_4 + \mathrm{OH} + \mathrm{CN}\ (74.28);\ 74.27$$

3.1.2. $Cu_2[W(CN)_2(OH)_2(C_2H_8N_2)(H_2O)_2]Cl_4$ II

The TG and DSC curves of II are shown in Fig. 3 and Fig. 4 respectively. The TG curve shows that the compound is thermally stable upto 140°C. The dehydration of the complex starts from 141°C upto 160°C with DTG maximum of 147.5°C which is due to removal of one mole of H_2O alongwith one mole of ethylenediamine. The expected endothermic peak for the dehydration process is shown from the DSC curve between the temperature range of 130°C to 179°C with maximum of 153.88°C. The enthalpy observed (ΔH) is 39.6 J/g. The decomposition of the remaining complex occurs in two steps. Second stage occurs in the temperature range of 247°C to 261°C, with DTG maximum at 255°C corresponding to the loss of another mole of water. The DSC curve displays an endothermic peak with temperature range of 378°C to 420°C with maximum of 383.0°C with an enthalpy change of ΔH=21.9 J/g. The third and the last stage in TG occurs between 278°C and 301°C and is due to the release of two moles of hydroxide. In the third transition of DSC an endothermic peak is displayed between 471°C and 496°C with maximum 484.2°C giving ΔH=5.0 J/g. The residue has the composition of 2CuCN+WCl_4 with the observed weight 79.51 against calculated 79.39%. The observed mass loss

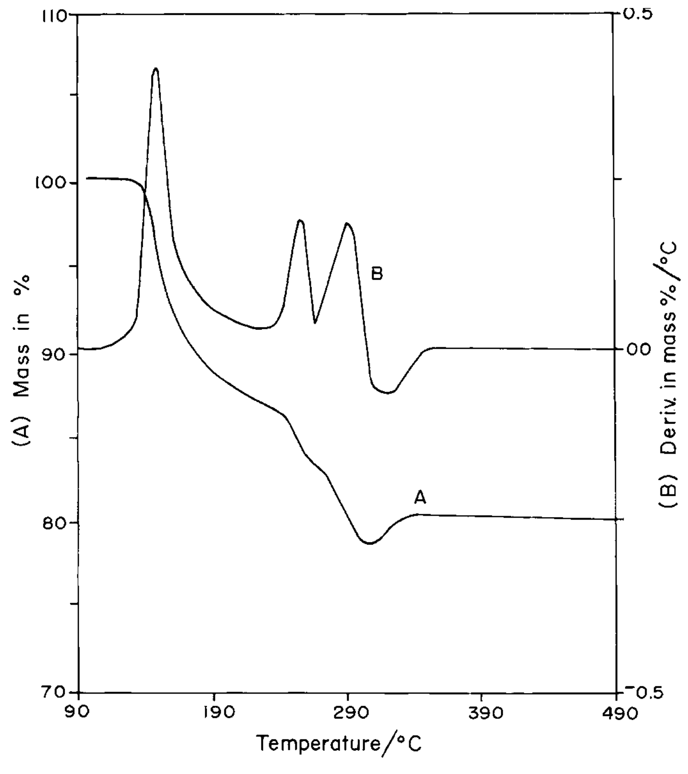

Fig. 3. The TG and DTG curve of complex II.

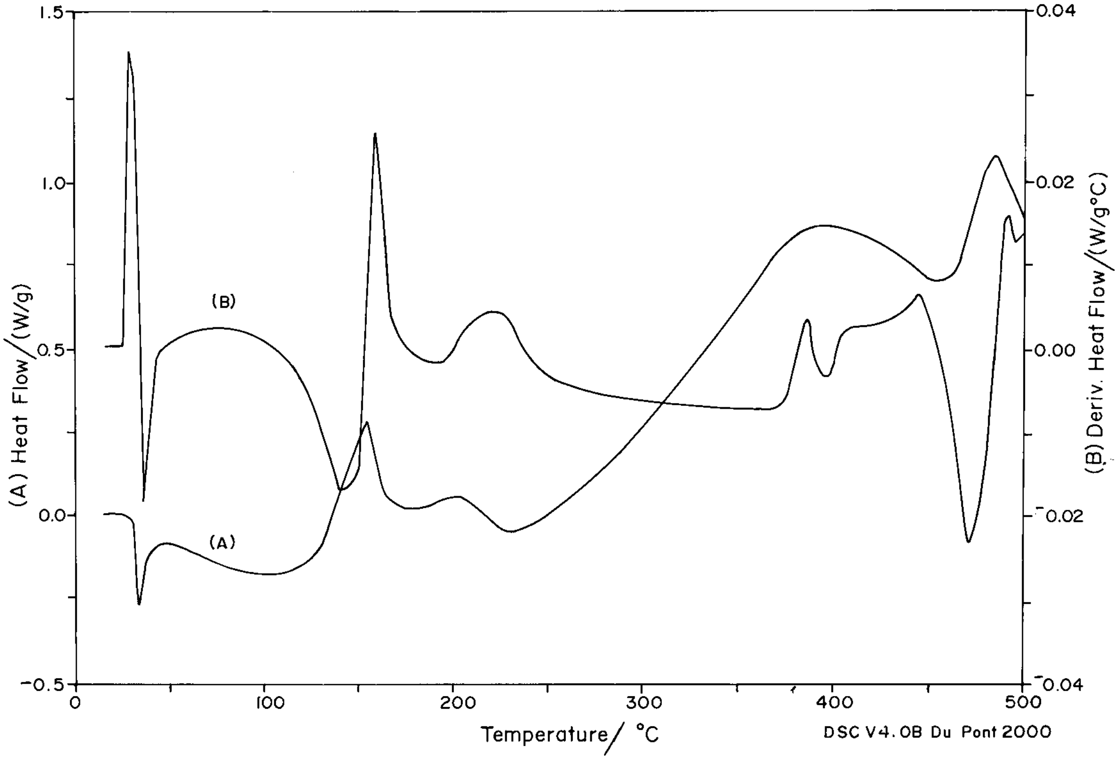

Fig. 4. The DSC curve of complex II.

percentage corresponds to the calculated values (Table 1). The decomposition temperature of CuCN in N_2 being 473°C justifies it as residue in decomposition processes of both the complexes. The scheme proposed to explain the thermal decomposition is shown as:

Scheme II

$$Cu_2[W(CN)_2(OH)_2(C_2H_8N_2)(H_2O)_2]\,Cl_4 \xrightarrow[12.16]{(12.28)}$$

$$Cu_2[W(CN)_2(OH)_2(H_2O)]Cl_4 + H_2O + C_2H_8N_2 \xrightarrow[3.47]{(2.83)}$$

$$Cu_2[W(CN)_2(OH)_2]Cl_4 + H_2O \xrightarrow[4.38]{(5.35)}$$

$$2CuCN + WCl_4 + 2OH\ (79.51);\ 79.39$$

3.2. Kinetic parameters

The kinetic parameters calculated using differential methods like Doyle, Coats and Redfern and Arrhenius for different stages of decomposition of I and II are listed in Tables 2 and 3 respectively. The form of these equations is given below:

Doyle′s method : (1)

$$\log\frac{\rho_T}{W} = \frac{E_a}{4.6T} + \log\frac{A}{RH}$$

where ρ_T: t/RH: $-\mathrm{d}w/\mathrm{d}t$: fraction decomposed at time t, W: weight of the sample at time 't', RH: heating rate, E_a: activation energy, A: frequency factor, T: temperature in kelvin.

Coats and Redfern method : (2)

$$\frac{\ln l - (1-\alpha)^{l-n}}{(1-n)T^2} = \ln\frac{AR}{\theta - E_a}\left[\left(1 - \frac{2RT}{E_a}\right)\right]\frac{E_a}{RT}$$

where α: fraction decomposed at time t, n: order of reaction, E_a: activation energy, θ: linear heating rate and R: gas constant

Table 2
Activation energy, frequency factor and entropy of activation for $Cu_2[Mo(CN)_2(OH)_2(C_2H_8N_2)(H_2O)_2]Cl_4$I

Stage	Parameters	DTG max. temp.in K	Doyle	Coats and Redfern	Arrhenius
I	E_a(kJ mol^{-1})		36.0	29.8	37.9
	A(s^{-1})	365.0	3.1	3.3	2.3
$\Delta S^{\#}$	(J k^{-1} mol^{-1})		−237.3	−236.9	−239.6
II	E_a(kJ mol^{-1})		41.8	33.5	41.7
	A(s^{-1})	411.7	3.7	2.9	2.7
	$\Delta S^{\#}$ (J k^{-1} mol^{-1})		−236.7	−238.9	−239.3
III	E_a(kJ mol^{-1})		34.4	28.9	38.1
	A(s^{-1})	464.3	2.8	3.5	2.2
	$\Delta S^{\#}$ (J k^{-1} mol^{-1})		240.1	−238.3	−242.0
IV	E_a(kJ mol^{-1})		18.6	14.0	23.5
	A(s^{-1})	614.0	0.9	5.3	0.4
	$\Delta S^{\#}$ (J k^{-1} mol^{-1})		−251.5	−237.1	−257.8

Table 3
Activation energy, frequency factor and entropy of activation for $Cu_2[W(CN)_2(OH)_2(C_2H_8N_2)(H_2O)_2]Cl_4$ II

Stage	Parameters	DTG max. temp. in K	Doyle	Coats and Redfern	Arrhenius
I	E_a(kJ mol^{-1})		15.7	8.7	16.9
	A(s^{-1})	420.5	0.8	5.7	0.008
	$\Delta S^{\#}$ (J k^{-1} mol^{-1})		−249.9	−233.4	−288.0
II	E_a(kJ mol^{-1})		20.4	12.5	24.4
	A(s^{-1})	528.5	1.2	5.3	0.7
	$\Delta S^{\#}$ (J k^{-1} mol^{-1})		−248.2	−235.8	−253.0
III	E_a (kJ mol^{-1})		22.9	15.3	22.3
	A(s^{-1})	562.4	1.3	5.1	0.5
	$\Delta S^{\#}$ (J k^{-1} mol^{-1})		−248.2	−236.7	−256.7

Arrhenius method : (3)

$$-\frac{dx}{dt} = kx^n$$

where x: amount of the sample undergoing reaction, n: order of the reaction and k: specific rate constant

The kinetic parameters were calculated by plotting the left hand side of Eqs. (1)–(3) against $1/T$ from which the values of E_a and A are calculated from the slope and intercept respectively (Figs. 5 and 6). The plot of each stage of the thermal decomposition of I and II gives linear graph showing the order as unity.

The entropy of activation ($\Delta S^{\#}$)was calculated from the equation:

$$A = \left(\frac{kT_s}{h}\right)\exp\left(\frac{\Delta S^{\#}}{R}\right) \qquad (4)$$

where k: Boltzmann constant; h: Planck's constant; ($\Delta S^{\#}$): entropy of activation. T_s : DTG peak temperature. In the case of I (Table 2), a higher value of activation energy (E_a) is observed in stage II, an intermediate value in stage I and a lower value in stage IV, the same trend holds good for pre-exponential factor A(s^{-1}) and entropy of activation($\Delta S^{\#}$) for all the methods involved. The values from Doyle's and Arrhenius methods are in close agreement with each other. In case of complex II (Table 3), higher activation energy E_a is observed in stage III, an intermediate value in stage II and lower energy value in stage I, the trend being the same with all other parameters and methods as well. Entropy of activation ($\Delta S^{\#}$) values for both the complexes are negative indicating a more ordered structure in the activated state than reactants and that the reactions are slower than the normal [19].

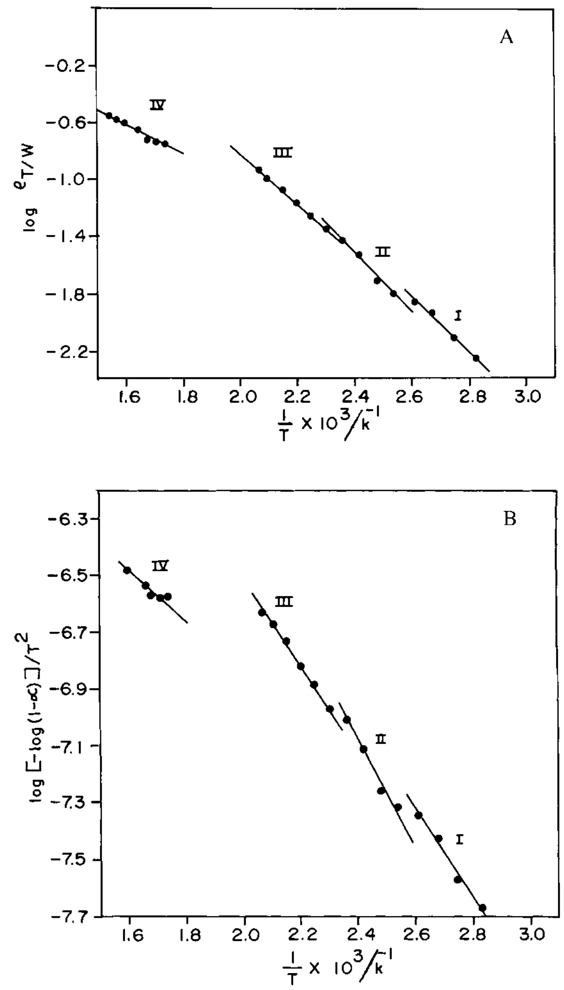

Fig. 5. (a) Plot of log ρ_T/w vs $1/T \times 10^3$ K^{-1} of complex I.(b) Plot of Log[$-\log(1-\alpha)$]/T^2 vs $1/T \times 10^3$ K^{-1} of complex I.

From the comparison of the kinetic parameters of the complexes, lower value of activation energy is observed in case of tungsten complexes showing great bonding between coordinating moeities and the tungsten atom in the complex [20].

Acknowledgements

One of the authors Kowsar Majid is grateful to CSIR, New Delhi for the award of Senior Research Fellowship.

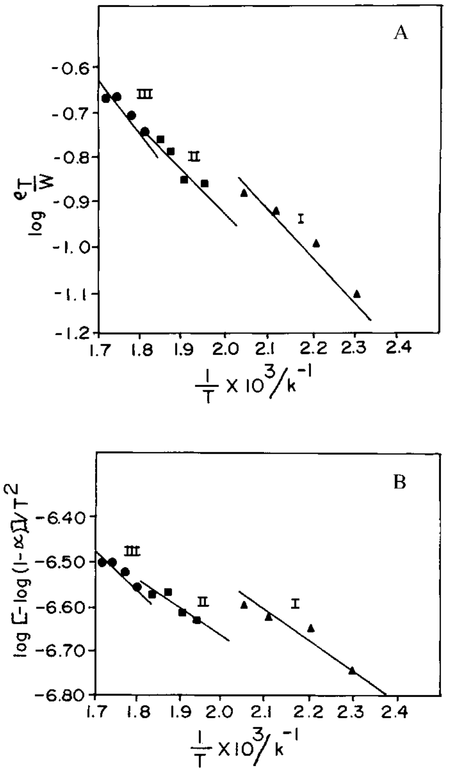

Fig. 6. (a) Plot of log ρ_T/w vs $1/T \times 10^3$ K^{-1} of complex II.(b) Plot of Log [$-\log(1-\alpha)$]/T^2 vs $1/T \times 10^3$ K^{-1} of complex II.

References

[1] J. Peisach, P. Asen, W. Blumberg (Eds.), The Biochemistry of Copper, Academic Press, New York, 1966.

[2] W.S. Hangarter, Inflammatory Disease and Copper, in: J.R.J. Sorensen (Ed.), Humana Press, Clifton, NJ, 1982, p. 439.

[3] S. Padhye, G.B. Kauffman, Coord. Chem. Rev. 63 (1985) 127.

[4] D.R. West, S.B. Padhye, P.B. Sonaware, Structure and Bonding 76 (1991) 1.

[5] J.R. Allan, G.H.W. Milburn, F. Richmond, Thermochim. Acta 170 (1990) 147–154.

[6] J.R. Allan, D.R. Vain, B.R. Caison, Thermochim. Acta 165 (1990) 201–206.

[7] J.R. Allan, G.H.W. Milburn, F. Richmond, D.L. Gereand, J. Birnie, A.S. Wilson, Thermochim. Acta 173 (1990) 185–191.

[8] H.S.O. Chan, T.S.A. Hor, J.R. Lusty, K.H. Lim, J. Therm. Anal. 34 (1988) 121–133.

[9] T.S. Andyhor, H.S.O. Chan, C.S.M. Chian, K.H. Lim, Thermochim. Acta 128 (1988) 175–184.

[10] V. Balzani, V. Carassiti, Photochemistry of Coordination Compounds, Academic Press, New York, 1970.

[11] R.P. Mitra, B.K. Sharma, H. Mohan, Aust. J. Chem. 25 (1972) 449.

[12] A.E. Nya, H. Mohan, Polyhedron 3 (1984) 743.

[13] S.I. Ali, N.K.S. Pundhir, J. Therm. Anal. 38 (1992) 1391.

[14] S.I. Ali, A.M.A. Ansari, J. Therm. Anal. 46 (1996) 1763.

[15] S.I. Ali, A.M.A. Ansari, N.K.S. Pundhir, Indian J. Chem. 34A (1995) 423.

[16] S.I. Ali, H. Kaur, Transition Met. Chem. 16 (1991) 450–453.

[17] L.G. Leipoldt, L.D.C. Bok, P.T.Z. Colliers, Z. Allg. Anorg. Chem. 407 (1974) 350, 409 (1974) 343–344.

[18] L. Gabelica, Spectrochimica Acta 32A (1976) 377.

[19] A.A. Frost, R.G. Pearson, Kinetics and Mechanism, Wiley, New York, 1961, p. 101.

[20] R. Lozano, A. Moragues, J. Roman, Thermochim. Acta 108 (1986) 1–7.